

Structures and Interaction Energies of Nucleic Acid Base–Amino Acid Complexes. Methylcytosines–Acrylamide Model

I. Galetich, S. G. Stepanian, V. Shelkovsky, M. Kosevich, Yu.P. Blagoi, and L. Adamowicz*

Department of Chemistry, University of Arizona, Tucson, Arizona 85721, and Institute for Low-Temperature Physics and Engineering, National Academy of Sciences of Ukraine, 47 Lenin Avenue, Kharkov 310164, Ukraine

Received: March 22, 1999; In Final Form: October 11, 1999

The interaction energies between the cytosine methylated derivatives ($m^1\text{Cyt}$, $m_2^{1,N}\text{Cyt}$, $m_3^{1,N,N}\text{Cyt}$) and acrylamide, which models the side chains of natural amino acids asparagine and glutamine, were measured using the temperature-dependent field ionization mass spectrometry method. The experimental enthalpies of the dimer formation are -57.0 kJ mol^{-1} for the acrylamide– $m^1\text{Cyt}$ dimer, -58.7 kJ mol^{-1} for the acrylamide– $m_2^{1,N}\text{Cyt}$ dimer and -45.7 kJ mol^{-1} for the acrylamide– $m_3^{1,N,N}\text{Cyt}$ dimer. The dimer structures were determined using quantum-chemical calculations. The calculated structures are almost planar with antiparallel orientations of the monomer dipoles and they are stabilized by intermolecular $\text{N–H}\cdots\text{O}$ and $\text{N–H}\cdots\text{N}$ H-bonds. The calculated interaction energies are in good agreement with the experimental data. The results indicate that the interaction energy between acrylamide and $m^1\text{Cyt}$ is significantly higher than that between acrylamide and $m^1\text{Uracil}$. This result is relevant to the mechanism of the protein–nucleic acid recognition.

1. Introduction

The protein–DNA interactions are among the most important biological processes. These types of interactions occur at all stages of the DNA replication and expression and in many processes of bioregulation. Despite this significant biological relevance there has been very little study of the molecular mechanisms of the protein–DNA interaction mainly due to large sizes of these systems and due to the complexity of the interaction effects. An important direction of the experimental investigations of complexes involving natural proteins and DNA concerns direct interactions between the nucleic acid bases and the amino acids forming side chains in the proteins. An example of a DNA–protein complex, where cytosine interacts via H-bonds with an amide amino acid side chain, is the complex of the bovine papilloma virus-1 E2 DNA binding domain of transcription protein with target viral DNA.¹ According to X-ray data, in this complex the Asn336 side chain of the E2 protein interacts with cytosine in the conservative triplet ACC of the complementary domain of DNA. The X-ray investigation of the specific “repressor–operator” complex of bacteriophage-434² allowed a direct identification of the H-bond interactions between the nucleic acid bases and the amide groups. NMR measurements³ confirmed the existence of the amino acid–nucleic acid base H-bonds. In the model study of the DNA–protein interactions,⁴ a destabilizing effect of acrylamide on DNA was recorded. This effect is caused by formation of H-bonds between the amide group and the nucleic bases in the single-strand regions. The study also demonstrated an important role of the part of the protein containing the amide group and its interaction via H-bonds with the DNA nucleic acid bases in untwisting the DNA double helix structure.

However, the above-mentioned studies have not allowed determination of how specific the interactions are between the

protein polar groups and the nucleic acid sites. To investigate this specificity experimental investigations of simpler model systems, which contain some characteristic structural feature of the DNA–protein systems, such as complexes of nucleic acid bases and compounds modeling amino acid side chains, are needed. These types of experiments may provide a more detail information on the structural and thermodynamic characteristics allowing better understanding and modeling of the DNA–protein interactions.

In the works belonging to this series of studies we use the method of the temperature-dependent field ionization (TD FI) mass spectrometry to determine the interaction energies between the nucleic acid bases and acrylamide ($\text{CH}_2=\text{CH}-\text{CO}-\text{NH}_2$), which models the amide side chain of the natural amino acids Asparagine and Glutamine. The main goal of these works has been the elucidation of the molecular mechanisms involved in the specific recognition of nucleic acid bases by amino acid side chains. A study of the interaction between the components of nucleic acids and protein fragments allows one to describe the role of different atomic groups in formation of protein–nucleic acid complexes. The TD FI mass spectrometry is one of a few methods whose result can be directly compared with the results of quantum-chemical calculations because both types of studies concern isolated systems. This approach has been successfully applied before in experimental determination of the formation energies of nucleic acid base dimers,⁵ as well as in determination of the formation energies of pair and triple complexes of nucleic bases with water molecules in a vacuum.^{6–11}

Recently we investigated the structural and thermodynamic characteristics of the 1-methyluracil ($m^1\text{Ura}$)–acrylamide dimers using the TD FI mass spectrometry and the quantum mechanical calculations.¹² In the calculations we determined the enthalpy of formation of the dimers and we showed that the MP2/6-31+G* and B3LYP/6-31++G** quantum mechanical calculations with accounting for the basis set superposition error (BSSE) corrections and the zero-point vibration energy (ZPVE)

* Corresponding author: E-mail: ludwik@u.arizona.edu. Fax: (520) 621-8407.

contributions provide interaction energies of the dimers in good agreement with the experimental results.

In the present work we describe an investigation of the structural and thermodynamic characteristics of the complexes formed by acrylamide with methyl derivatives of cytosine. These derivatives are 1-methylcytosine ($m^1\text{Cyt}$), 1, N -dimethylcytosine ($m_2^{1,N}\text{Cyt}$), and 1, N,N -trimethylcytosine ($m_3^{1,N,N}\text{Cyt}$). The complexes of acrylamide with these methylated cytosines model interaction between the amide group of amino acids with the functional groups of cytosine which are free and open to interaction in the helical and unfolded states of the nucleic acids. Acrylamide is a suitable model of the amino acid amide group ($-\text{CO}-\text{NH}_2$). The calculations of acrylamide and Glutamine performed at the DFT/B3LYP/6-31++G** level of theory demonstrated almost identical electronic and structural parameters of the amide group in these molecules. This indicates that their H-bonding properties should also be very similar. For example, the charges of the amide group atoms in acrylamide and glutamine (acr/Glu) are oxygen, $-0.50/-0.50$; carbon, $-0.21/0.22$; nitrogen, $-0.54/-0.50$; hydrogen (cis), $-0.33/0.34$; and hydrogen (trans) $0.31/0.29$. The distance between the amide group atoms directly involved in the intermolecular H-bonding (O and H(cis)) is 2.503 \AA in acrylamide and 2.501 \AA in glutamine. These data confirm that the amide groups in acrylamide and glutamine are very similar. On the other hand, the vapor pressure of acrylamide is similar to the vapor pressures of nucleic acid bases and their methylated derivatives, which is another reason this compound was chosen for the present study. In the mass-spectrometry experiment on the gas-phase acrylamide-base dimerization it is very important to obtain a gaseous mixture with approximately equal concentrations of the two components, and this is easier to achieve when the two have similar vapor pressure. Another advantage of using acrylamide in the study is that this compound appears only in a single conformation in the gas phase, and this fact simplifies both the analysis of the experimental spectra and the calculations.

It is of great practical interest whether the interaction energy between the protein amide group and cytosine is different than the interaction energy between the amide group and uracil. If these energies are different it would allow the amide group to more specifically target one of the bases and avoid the other. This phenomenon will constitute the base for the chemical "recognition" of the DNA and RNA bases by the protein.

In applying the field ionization technique one should be aware that the electric field, which is imposed on an equilibrium mixture of monomers and dimers in the experiment, may affect the thermodynamic equilibrium between the monomers and the dimers and influence the experimental results. In the present work we have investigated this influence and we have demonstrated that the results can be extrapolated to the zero field to obtain field-free interaction energy values.

2. Experimental Method

The use of the method of the temperature-dependent field ionization mass spectrometry to determine the enthalpies of association of molecules in the gas phase, was described in details elsewhere.^{6,12} The main features of the method are as follows. Gas-phase mixture of the molecules under study is generated in the reactive zone (separated by a cylindrical counter electrode) of the field ionization ion source; the molecular flows of the two compounds, whose complexes are investigated, are generated by evaporation of crystalline samples from two heated Knudsen-type glass cells. The gas pressure achieved in the

reaction zone is usually sufficient for the formation of hydrogen-bonded or van der Waals associates. The pressure (expressed in terms of the number of molecules per cm^3) can be determined using the barometric equation

$$n(F) = n_0(T) \exp[(\mu F + (\alpha/2)F^2)/kT]$$

where the symbols used in the equation indicate the following quantities: μ the dipole moment, α the polarizability, and F the emitter potential. In the case of the nucleic acid bases and their methylated derivatives, the density, $n(F)$, calculated for the temperature range of $300\text{--}400\text{ K}$ is $\approx 10^{19}\text{--}10^{20}$ molecules/ cm^3 . (At F_0 the density $n_0(T)$ was determined using the vapor pressure and the heat of sublimation.)

The hydrogen-bonded or van der Waals associates formed in the reaction zone are not destroyed under the soft-ionization conditions of the field ionization used in the TD FI experiment.^{6,13} The intensities of the ion currents (i.e., the intensities of the corresponding peaks in the mass spectrum) are proportional to the concentrations of the monomers and their associates in the gas-phase mixture. On this basis the association constants K_{ass} can be determined. The variation of the mass spectra with the temperature of the reactive mixture allows determination of the temperature dependencies of K_{ass} 's and construction of the van't Hoff's plots. The enthalpies of association can be calculated from these plots.

The mass-spectrometric measurements were performed using the MI-1201 mass spectrometer (Electron Works, Sumy, Ukraine) equipped with the laboratory ion source and described elsewhere.⁷ The details of the experimental procedure were presented in the previous paper of this series.¹² In addition to the already provided information, we should add the following to describe the technique used to achieve the desired temperature of the sample and the technique used in determining the field dependencies of the ion currents in the mass spectra. Electrolytically etched tungsten needles were used as the field ionization emitters. The resistive heating of the emitter by the $0\text{--}1.2\text{ A}$ electric current allowed changing the reactive zone temperature from 20 to $150\text{ }^\circ\text{C}$. The experiments were performed at the emitter potential of $5, 4, 3$, and 2.5 kV in order to determine the field dependency of the mass spectra. Measurements at field strengths lower than that provided by the emitter potential of 2.5 kV was impossible due to a too low efficiency of the ionization and a very low ion current of the complex. The three methyl derivatives of cytosine, $m^1\text{Cyt}$, $m_2^{1,N}\text{Cyt}$, $m_3^{1,N,N}\text{Cyt}$, were synthesized at the Kharkov State University (Ukraine). Acrylamide was purchased from Reanal, Hungary.

3. Computational Details

In the present study, the interaction energies between acrylamide and the methylated cytosines have been calculated using the MP2 (Møller–Plesset second-order perturbation theory)^{14,15} and DFT (density functional theory) methods. The DFT method was also employed in the calculations of the IR frequencies using the harmonic approximation. The frequencies were used to determine the ZPVE corrections. The DFT calculations were carried out with the three-parameter density functional, usually abbreviated as B3LYP, which includes Becke's gradient exchange correction,¹⁶ the Lee, Yang, Parr correlation functional,¹⁷ and the Vosko, Wilk, and Nusair correlation functional.¹⁸

In the first step of the calculations, the geometries of the acrylamide- $m^1\text{Cyt}$ and acrylamide- $m_2^{1,N}\text{Cyt}$ dimers were optimized at the MP2/6-31+G* level of theory, and for each of these systems a single equilibrium structure was found. The

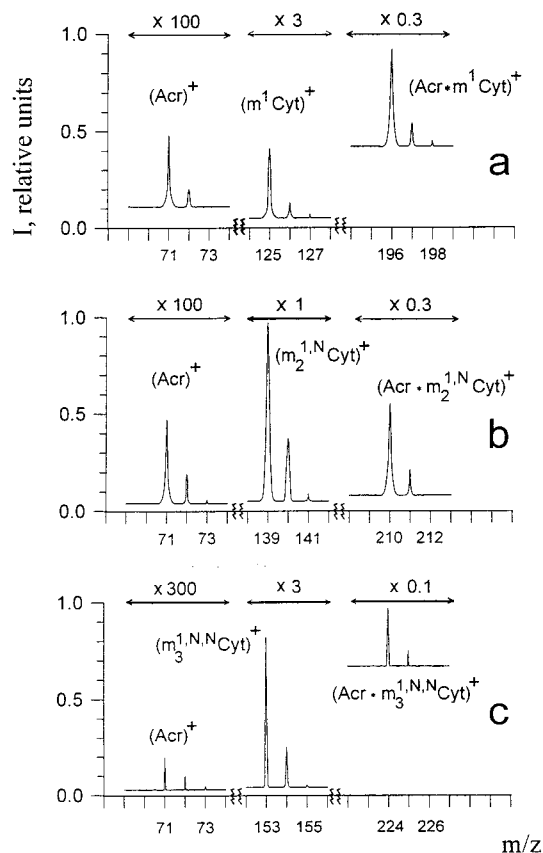


Figure 1. Field ionization mass spectra of the reaction mixture of acrylamide with (a) $m^1\text{Cyt}$, (b) $m_2^{1,N}\text{Cyt}$, and (c) $m_3^{1,N,N}\text{Cyt}$. Emitter potential $U = +5$ kV. Emitter temperature $T = 298$ K.

MP2/6-31+G* optimal geometries were used to calculate the MP2/6-31++G** energies of the dimers. Next the geometries of the dimers were reoptimized at the DFT/B3LYP/6-31++G** level and the DFT harmonic frequencies were calculated. DFT/B3LYP/6-31++G** optimizations were also carried out for the acrylamide– $m_3^{1,N,N}\text{Cyt}$ and two equilibrium structures were found. These results will be discussed in the next section. The interaction energies of the dimers were estimated with accounting for BSSE using the counterpoise method of Boys and Bernardi.¹⁹ All calculations in this work were done on IBM RS6000 workstations using the Gaussian94 quantum-chemical program package.²⁰

4. Results and Discussion

Enthalpies of Formation. First we carried out experiments at the emitter potential of +5 kV and the emitter temperature of 298 K. The field ionization mass spectra of acrylamide and the three methyl derivatives of cytosine ($m^1\text{Cyt}$, $m_2^{1,N}\text{Cyt}$, $m_3^{1,N,N}\text{Cyt}$) obtained at these conditions are presented in Figure 1. They are qualitatively similar to the earlier reported spectrum of the acrylamide– $m^1\text{Ura}$ mixture.¹² In the spectra in Figure 1 one easily identifies the peaks corresponding to the ions of the monomers and the ions of their associates. Using the intensities of the spectra peaks corresponding to the monomers ($I_{[\text{Base}]}$ and $I_{[\text{Acr}]}$) and the dimer ($I_{[\text{Acr} \cdot \text{Base}]}$) we calculated the association constant (K_{ass}) using the following equation:

$$K_{\text{ass}} = I_{[\text{Acr} \cdot \text{Base}]} / I_{[\text{Acr}]} I_{[\text{Base}]}$$

Next, we repeated the experiments at the different emitter temperatures mentioned in the Experimental Section to determine the temperature dependencies of the K_{ass} 's. The mass

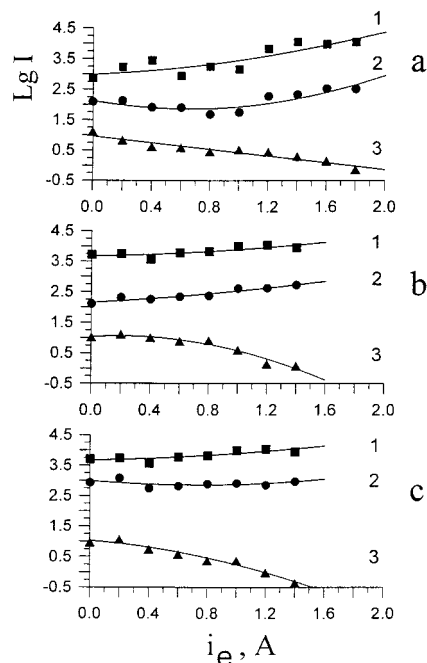


Figure 2. Dependencies of the ion currents (I) vs currents of the emitter resistive heating (I_e) for acrylamide (1), methylated cytosine (2), and their dimer (3). (a) $m^1\text{Cyt}$, (b) $m_2^{1,N}\text{Cyt}$, (c) $m_3^{1,N,N}\text{Cyt}$. Emitter potential $U = +5$ kV.

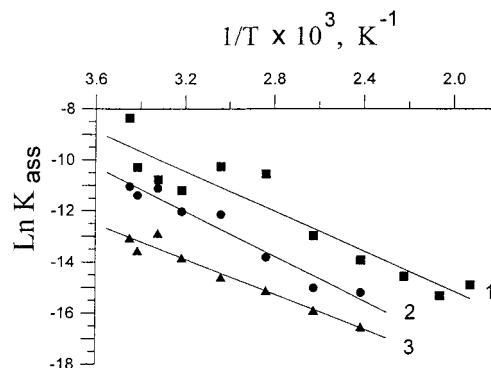


Figure 3. Temperature dependencies of the K_{ass} for (1) acrylamide– $m^1\text{Cyt}$, (2) acrylamide– $m_2^{1,N}\text{Cyt}$, and (3) acrylamide– $m_3^{1,N,N}\text{Cyt}$ dimers. Emitter potential $U = +5$ kV.

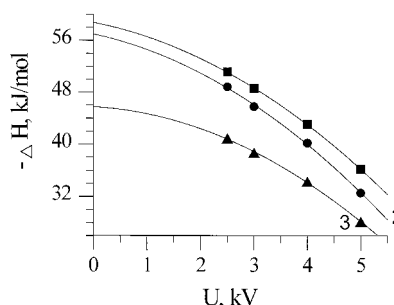
spectra showed a decrease of the peak intensities corresponding to the dimers with increasing temperature. The dependencies of the peak intensities on the temperature in the reactive zone were measured as the dependency of the ion current on the magnitude of the electric current in the resistive heating element of the emitter. The results of the measurements are shown in Figure 2. Using these data we calculated K_{ass} 's for the three studied systems and generated the van't Hoff's plots, which show the temperature dependencies of the logarithms of the association constants. The plots obtained at the emitter potential of +5 kV are presented in Figure 3.

In determining the enthalpies of the dimer formation of the methylated cytosines with acrylamide, we had to consider the dependence of the enthalpies on the field strength which was observed in our previous study on the cytosine homodimers.²¹ That study also showed a correlation between the field-dependent enthalpy values and the dipole moment of cytosine and its dimer with acrylamide. The correlation was explained by the “stretching” effect of a nonhomogeneous electric field (created by field ionization emitter) on the dimerization of polar molecules. The degree of the alignment of the monomer dipoles

TABLE 1: Total Energies (au), Interaction Energies (IE, kJ mol⁻¹) and Zero-Point Vibration Energies (ZPVE, au) of the Acrylamide–m¹Cyt, Acrylamide–m₂^{1,N}Cyt and Acrylamide–m₃^{1,N,N}Cyt Dimers Calculated at the DFT/B3LYP/6-31++G Level of Theory and the Experimentally Determined Enthalpies of Formation (ΔH) of These Complexes^a**

	acrylamide–m ¹ Cyt	acrylamide–m ₂ ^{1,N} Cyt	acrylamide–m ₃ ^{1,N,N} Cyt	
			dimer A	dimer B
energy	–681.620 072	–720.929 212	–760.226 039	–760.226 431
IE	65.8	66.7	38.7	39.7
ZPVE ^b	0.197 275	0.224 090	0.249 905	0.249 993
ZPVE correction	0.002 623	0.002 560	0.001 908	0.001 997
BSSE correction ^c				
acrylamide	0.000 489	0.000 528	0.000 323	0.000 283
methylated cytosine	0.000 483	0.000 413	0.000 387	0.000 491
total	0.000 972	0.000 941	0.000 710	0.000 774
IE (BSSE corrected)	63.3	64.2	36.8	37.7
IE (BSSE and ZPVE corrected)	56.4	57.5	31.8	32.5
– ΔH , kJ mol ⁻¹	57.0	58.7		45.7
μ , D ^d	6.44	6.61		6.12

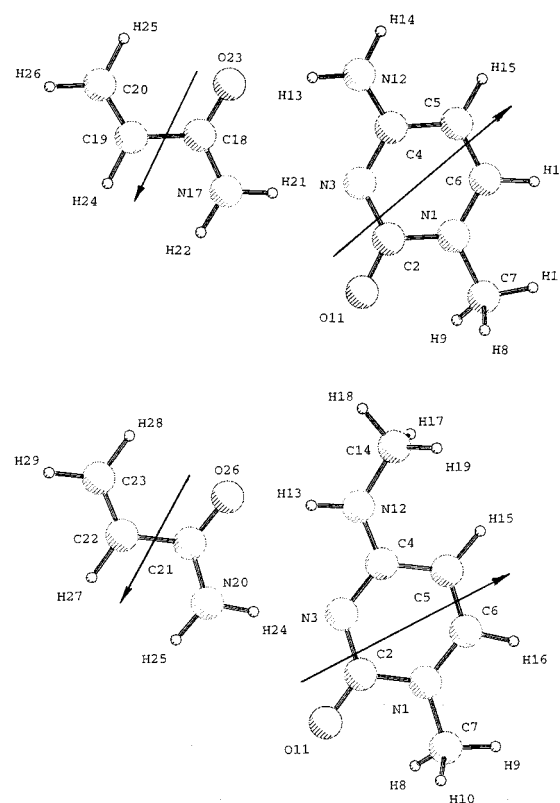
^a All calculated energies were obtained for the dimer geometries optimized at the DFT/B3LYP/6-31++G** level of theory. ^b Calculated based on the DFT/B3LYP/6-31++G** frequencies scaled by the factor of 0.95. ^c Energy difference calculated for the equilibrium monomer geometries in the monomer and dimer basis sets. ^d Dipole moments of the monomer methylcytosines calculated at the DFT/B3LYP/6-31++G** level of theory.

**Figure 4.** Field dependencies of the enthalpies of formation of the (1) acrylamide–m₂^{1,N}Cyt, (2) acrylamide–m¹Cyt, and (3) acrylamide–m₃^{1,N,N}Cyt dimers.

along the direction of the field contributes to stabilization or destabilization of the dimer. In particular, the destabilization effect is the strongest when dimers with an antiparallel orientation of the dipole vectors of the monomers are formed, because this type of orientation is unfavorable when an electric field is imposed on the sample. A detailed study of the destabilizing effect in field ionization experiments was performed earlier.²² It should be noted that in the study of the acrylamide–m¹Uracil dimer¹² no field dependencies were observed, which were attributed to a relatively low value of the uracil dipole moment (of about 4 D). However, due to a higher dipole moment of cytosine, the formation enthalpy of its dimer with acrylamide shows a more noticeable field dependency.

To further elucidate the field effect on the enthalpy of the dimer formation, we performed the following additional experiments. Mass spectra were measured for all the considered systems at different values of the emitter potential (4, 3, and 2.5 kV) resulting in different field strengths being imposed on the sample. For the value of the emitter potential, we calculated the enthalpies of formation. As expected, in contrast to other nucleic acid bases studied before,^{12,22} the dimerization enthalpies of the methylated cytosines and acrylamide showed some field dependency, which is illustrated in Figure 4. We extrapolated these plots to the zero field, and the results are presented in Table 1.

Structures of the Dimers. Both the B3LYP/6-31++G** and MP2/6-31+G* calculations predicted almost planar single structures for the acrylamide–m¹Cyt and acrylamide–m₂^{1,N}Cyt dimers. The structures are shown in Figure 5. As it is seen, the dimers are connected by N–H···O and N–H···N H-bonds.

**Figure 5.** Equilibrium geometries of the (top) acrylamide–m¹Cyt and (bottom) acrylamide–m₂^{1,N}Cyt dimers calculated at the MP2/6-31+G* level of theory. (The geometries of the dimers are available from the corresponding author.)

The two acrylamide–m₃^{1,N,N}Cyt dimers found in the DFT/B3LYP/6-31++G** calculations are denoted as *Dimer A* and *Dimer B* are shown in Figure 6. These dimers are stabilized by the conventional N–H···OH-bond and by a weak interaction between the acrylamide oxygen and the methyl group of m₃^{1,N,N}Cyt. The calculated dipole moment vectors of the acrylamide and methylated cytosine monomers shown in Figure 5 are almost antiparallel in both dimers and the resulting dimer dipole moments are significantly lower than the dipole moments of the m¹Cyt and m₂^{1,N}Cyt monomers (6.44 and 6.61 D, respectively, vs 3.51 and 3.49 D for the corresponding dimers). This finding is consistent with the field dependency of the enthalpies of the dimer formation observed in the TD FI experiments and

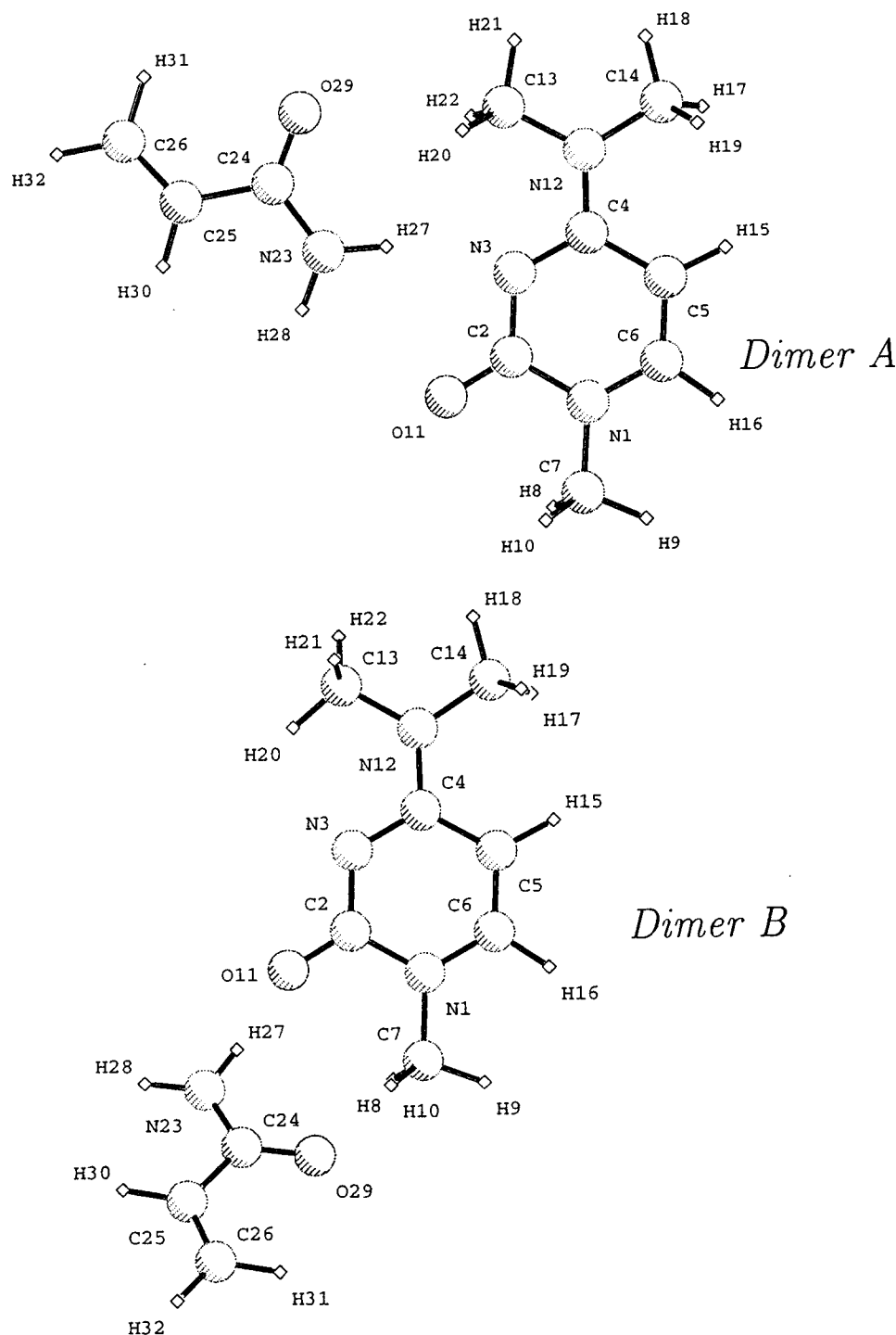


Figure 6. Equilibrium geometries of the (top) acrylamide– $m_3^{1,N,N}$ Cyt *Dimer A* and (bottom) *Dimer B* structures calculated at the DFT/B3LYP/6-31++G** level of theory. (The geometries of the dimers are available from the corresponding author.)

presented in Figure 4, since the lower dipole moments of the dimers than those of the monomers should result in higher stabilization of the monomers than the dimers in the field, and in an effective lowering of the dimerization enthalpies. In the case of the m^1 Ura–acrylamide dimer studied before, where no field dependency on the dimerization enthalpy was observed, the situation was different. The calculated dipole moment of the m^1 Ura monomer of 5.14 D was similar to the dipole moment of one of the two almost equally stable dimers which m^1 Ura forms with acrylamide (the calculated values of the dipole moments of the dimers were 5.72 and 2.79 D). In such a case, when the electric field is turned on, the dimer with the higher dipole moment becomes more thermodynamically stable and it

will be produced in higher quantities than the dimer with the smaller dipole moment. However, this effect cannot be detected by the TD FI mass spectrometry, since this method cannot distinguish between different structural conformers. Moreover, since m^1 Ura and one of the m^1 Ura–acrylamide dimers have similar dipole moments, the field stabilization effects for both systems are similar and no noticeable change in the dimerization enthalpy should be observed when the field strength is increased. This explains the difference in the field dependence in the dimerization of the methylated uracil and the methylated cytosines with acrylamide.

The above interpretation of the field destabilizing effect for the methylated cytosines–acrylamide dimerization is further

TABLE 2: Total Energies (au), Interaction Energies (IE, kJ mol⁻¹) and Zero-Point Vibration Energies (ZPVE, au) of the Acrylamide–m¹Cyt and Acrylamide–m₂^{1,N}Cyt Dimers Calculated at the MP2/6-31+G* Level of Theory^a

	acrylamide–m ¹ Cyt	acrylamide–m ₂ ^{1,N} Cyt
energy	–679.540 780	–718.701 775
IE	75.8	80.6
ZPVE ^b	0.197 275	0.224 090
ZPVE correction	0.002 623	0.002 560
BSSE correction ^c		
acrylamide	0.002 809	0.003 163
m ¹ Cyt or m ₂ ^{1,N} Cyt	0.002 565	0.002 774
total	0.005 374	0.005 938
IE (BSSE corrected)	61.7	65.0
IE (BSSE and ZPVE corrected)	54.8	58.3

^a All Energies, except for the ZPVE, were obtained for the dimer geometries optimized at the MP2/6-31+G* level. ^b Calculated based on the DFT/B3LYP/6-31++G** frequencies scaled by the factor of 0.95. ^c Energy difference calculated for the equilibrium monomer geometries in the monomer and dimer basis sets.

TABLE 3: Total Energies (au), Interaction Energies (IE, kJ mol⁻¹) and Zero-Point Vibration Energies (ZPVE, au) of the Acrylamide–m¹Cyt and Acrylamide–m₂^{1,N}Cyt Dimers Calculated at the MP2/6-31++G Level of Theory^a**

	acrylamide–m ¹ Cyt	acrylamide–m ₂ ^{1,N} Cyt
energy	–679.641 237	–718.816 655
IE	73.9	78.8
ZPVE ^b	0.197 275	0.224 090
ZPVE correction	0.002 623	0.002 560
BSSE correction ^c		
acrylamide	0.002 380	0.002 744
m ¹ Cyt or m ₂ ^{1,N} Cyt	0.002 330	0.002 661
total	0.004 710	0.005 406
IE (BSSE corrected)	61.6	64.6
IE (BSSE and ZPVE corrected)	54.7	57.9

^a All Energies, except for the ZPVE, were obtained for the dimer geometries optimized at the MP2/6-31+G* level of theory. ^b Calculated based on the DFT/B3LYP/6-31++G** frequencies scaled by the factor of 0.95. ^c Energy difference calculated for the equilibrium monomer geometries in the monomer and dimer basis sets.

supported by the correlation between the dipole moments of the different methylated cytosines and the field dependency of the dimerization enthalpies. m₃^{1,N,N}Cyt has the lowest dipole moment among the cytosine derivatives studied (6.12 D, Table 1), and the formation enthalpy of its dimer with acrylamide decreases by 12.7 kJ mol⁻¹ when the emitter potential is changed from 2.5 to 5 kV. In the case of m¹Cyt and m₂^{1,N}Cyt, which have higher dipole moments (6.44 and 6.61 D, respectively), the enthalpy decreases are higher and equal to 16.2 and 15.0 kJ mol⁻¹, respectively.

Interaction Energies. As mentioned single structures of the acrylamide–m¹Cyt and acrylamide–m₂^{1,N}Cyt dimers were determined in the calculations. Both dimers are almost planar; the largest deviation from the planarity of approximately 15° occurs in the amino group. The two dimers have similar structures, i.e., the same groups are involved in the intramolecular H-bonding. The DFT/B3LYP/6-31++G** and MP2/6-31+G* methods predict very similar geometry parameters for the two systems. As expected, the most significant differences between the DFT and MP2 geometries occur in the lengths of the H-bonds. The DFT method predicts shorter lengths of these bonds than the MP2/6-31+G* method: 1.934 Å (N3···H21), 1.832 Å (H13···O23) at the DFT level vs 1.953 and 1.877 Å at the MP2 level (results for the acrylamide–m¹Cyt dimer).

The total energies, the ZPVEs, the BSSE corrections, and the interaction energies for the dimers calculated at the DFT/B3LYP/6-31++G** and MP2/6-31+G* levels are presented in Tables 1 and 2, respectively. The analysis of the data shows that the DFT and MP2 methods predict very similar interaction energies for both acrylamide–m¹Cyt and acrylamide–m₂^{1,N}Cyt dimers, when the BSSE and ZPVE corrections are accounted for. The difference between the methods is less than 2 kJ mol⁻¹. The calculated interaction energies are in good agreement with

the experimental enthalpies of formation of the dimers. The calculations and the experiment are in agreement in showing that the interaction between acrylamide and m₂^{1,N}Cyt is slightly stronger than the acrylamide–m¹Cyt interaction. The experimental energy difference is 1.7 kJ mol⁻¹, and the calculated differences are 3.15 kJ mol⁻¹ and 0.73 kJ mol⁻¹ at the MP2/6-31+G* and DFT/6-31++G** levels, respectively. As seen from Table 1, the interaction energies between acrylamide and m₃^{1,N,N}Cyt is considerably lower than in the acrylamide complexes with m¹Cyt and m₂^{1,N}Cyt. This is not surprising since acrylamide and m₃^{1,N,N}Cyt due to sterical constraints can only form one H-bond. The interaction energies in acrylamide–m₃^{1,N,N}Cyt *Dimer A* and *Dimer B* are almost identical (see Table 1), and they both may exist in the gas phase.

An important result of the present study is showing that the enthalpy of formation of the acrylamide–m¹Cyt dimer (58.7 kJ mol⁻¹) is much higher than for the acrylamide–m¹Ura dimer (40.6 kJ mol⁻¹).¹² This is an unexpected result because each of the dimers is stabilized by two similar H-bonds. The higher enthalpy of formation of the acrylamide–m¹Cyt dimer may be due to the proximity of the carbonyl oxygen, O11, of cytosine to the acrylamide amino group (see Figure 5). Although the O11···H21 distance in this system is longer than a conventional H-bond, it apparently provides additional stabilization to the acrylamide–m¹Cyt dimer.

5. Conclusions

In this work we have investigated the interaction energies and the structures of dimers of acrylamide with methylated cytosines. A good agreement was found between the experimental enthalpies of formation of the dimers obtained by means of the temperature-dependent field ionization mass spectrometry

method and the enthalpies predicted by the DFT/B3LYP/6-31++G** and MP2/6-31+G* methods with accounting for the BSSE and ZPVE corrections.

We found that the interaction of acrylamide, which models the amide side chain of the natural amino acids asparagine and glutamine, with m¹Cyt much higher (by ca. 50%) than with m¹Ura. This difference should allow the peptide amide group to distinguish between these two pyrimidine bases. It also explains the acrylamide recognition ability in the protein–DNA interface.

Acknowledgment. This work was supported by the NATO Grant CRG 973389 allowing the visit of Dr. S. G. Stepanian to the University of Arizona.

References and Notes

- (1) Hedge, R. S.; Grossman, S. R.; Lainins, L. A.; Sigler, P. B. *Nature* **1992**, 359, 505.
- (2) Anderson, J. E.; Ptashne, M.; Harrison, S. C. *Nature* **1987**, 326, 846.
- (3) Helene, C.; Lancelot, G. *Prog. Biophys. Mol. Biol.* **1982**, 39, 1.
- (4) Smolyaninova, T. I.; Bruskov, V. I.; Kashparova, E. V. *Mol. Biol. (Russ.)* **1985**, 19, 992.
- (5) Sukhodub, L. F.; Yanson, I. K. *Nature* **1976**, 264, 245.
- (6) Verkin, B. I.; Yanson, I. K.; Sukhodub, L. F.; Teplitsky, A. B. *Interactions of Biomolecules. New Experimental Approaches and Methods*; Naukova Dumka: Kiev, 1985 (in Russian).
- (7) Sukhodub, L. F.; Yanson, I. K.; Shelkovsky, V. S.; Wierchowsky, K. L. *Biophys. Chem.* **1982**, 15, 149.
- (8) Sukhodub, L. F.; Shelkovsky, V. S.; Wierchowsky, K. L. *Biophys. Chem.* **1984**, 19, 191.
- (9) Sukhodub, L. F.; Yanson, I. K.; Shelkovsky, V. S. *Stud. Biophys.* **1982**, 87, 223.
- (10) Poltev, V. I.; Kosevich, M. V.; Shelkovsky, V. S.; Pashinskaya, V. A.; Gonzales, E. A.; Teplukhin, A. V.; Malenkov, G. G. *Mol. Biol.* **1995**, 29, 220.
- (11) Sukhodub, L. F. *Chem. Rev.* **1987**, 87, 589.
- (12) Galetich, I.; Kosevich, M.; Shelkovsky, V.; Stepanian, S. G.; Blagoi, Yu. P.; Adamowicz, L. *J. Mol. Struct.* **1999**, it 478, 155.
- (13) Bekey, H.-D. *Principles of Field Ionization and Field Desorption Mass Spectrometry*; Pergamon: London, 1977.
- (14) Binkley, J. S.; Pople, J. A. *Int. J. Quantum Chem.* **1975**, 9, 229.
- (15) Pople, J. A.; Binkley, J. S.; Seeger, R. *Int. J. Quantum Chem., Quantum. Chem. Symp.* **1976**, 10, 1.
- (16) Becke, A. D. *Phys. Rev. B* **1988**, 38, 3098.
- (17) Lee, C.; Yang, W.; Parr, R. G. *Phys. Rev. B* **1988**, 37, 785.
- (18) Vosko, S. H.; Wilk, L.; Nusair, M. *Can. J. Phys.* **1980**, 58, 1200.
- (19) Boys, S. F.; Bernardi, F. *Mol. Phys.* **1970**, 19, 553.
- (20) Frisch, M. J.; Trucks, G. W.; Schlegel, H. B.; Gill, P. M. W.; Johnson, B. G.; Robb, M. A.; Cheeseman, J. R.; Keith, T.; Petersson, G. A.; Montgomery, J. A.; Raghavachari, K.; Al-Laham, M. A.; Zakrzewski, V. G.; Ortiz, J. V.; Foresman, J. B.; Cioslowski, J.; Stefanov, B. B.; Nanayakkara, A.; Challacombe, M.; Peng, C. Y.; Ayala, P. Y.; Chen, W.; Wong, M. W.; Andres, J. L.; Replogle, E. S.; Gomperts, R.; Martin, R. L.; Fox, D. J.; Binkley, J. S.; Defrees, D. J.; Baker, J.; Stewart, J. P.; Head-Gordon, M.; Gonzalez, C.; Pople, J. A. *Gaussian 94*, Revision E.2; Gaussian, Inc.: Pittsburgh, PA, 1994.
- (21) Yanson, I. K.; Teplitsky, A. B.; Sukhodub, L. F. *Biopolymers* **1979**, 18, 1149.
- (22) Teplitsky, A. B.; Galetich, I. K.; Sukhodub, L. F. *Mol. Biol. (Russ.)* **1990**, 25, 709.